Anomalous diffusion of proteins in sheared lipid membranes

Atefeh Khoshnood and Mir Abbas Jalali*

Computational Mechanics Laboratory, Department of Mechanical Engineering,
Sharif University of Technology, Azadi Avenue, Tehran, Iran.

We use coarse grained molecular dynamics simulations to investigate diffusion properties of sheared lipid membranes with embedded transmembrane proteins. In membranes without proteins, we find normal in-plane diffusion of lipids in all flow conditions. Protein embedded membranes behave quite differently: by imposing a simple shear flow and sliding the monolayers of the membrane over each other, the motion of protein clusters becomes strongly superdiffusive in the shear direction. In such a circumstance, subdiffusion regime is predominant perpendicular to the flow. We show that superdiffusion is a result of accelerated chaotic motions of protein–lipid complexes within the membrane voids, which are generated by hydrophobic mismatch or the transport of lipids by proteins.

Lipid bilayers constitute the main body of the cell membrane while being found in different organelles inside the cell. The cell membrane hosts collections of proteins and lipid rafts and it is crowded with a variety of biomolecules. In such non-homogenous and diverse environments, the diffusion of protein molecules in lipid bilayers plays a vital role in different biological processes like cell signaling. The diffusion of lipids and proteins is not a distinct phenomenon and depends on the environment and neighboring molecules [1], and even changes from cell to cell [2]. Transmembrane proteins diffuse as dynamic complexes with lipids [3, 4], and their interactions with lipid molecules mediates traffic in cell membranes. Experiments show that the hydrophobic mismatch between proteins and lipids controls the diffusion coefficient of molecules inside a bilayer [5, 6].

Anomalous sub- and super-diffusion processes are more efficient scenarios for finding a nearby target than normal diffusion [7, 8], and they enhance the formation of protein complexes and signal propagation. According to experiments, the mean square displacement (MSD) of membrane channel proteins of human kidney cell exhibits subdiffusion [9]. The addition of cholesterols to lipid membranes [10], and the augmented area coverage of membrane proteins [11] also lead to subdiffusion of lipids and proteins. Superdiffusivity has been observed in several physical systems [12, 13]. A recent study by Köhler et al. [14] shows that in a gel composed of actin filaments, fascin molecules and myosin-II filaments, the diffusion of small actin and fascin clusters are superdiffusive because of the work done by molecular motors.

In many conditions membranes are under shear. When a red blood cell (RBC) migrates through vessels smaller in diameter than itself, the RBC membrane is under shear. The blood flow exerts tangential shear stresses on vascular endothelia, and initiates cellular processes like activating G protein-coupled receptors. These receptors are able to sense the fluid shear stress as an increase in the lateral membrane tension, and subsequently go through conformational changes [15]. The temporal and spatial changes in the membrane fluidity, in response to shear flow, have been observed experimentally [16, 17].

In this study we are interested in the diffusivity of lipid and protein molecules in flat membranes under shear flow, and attempt to answer three fundamental questions using molecular dynamics (MD) simulations: (i) Do lipid and protein molecules have different diffusion properties parallel and perpendicular to flow direction? (ii) How does a simple shear flow influence the random motions of transmembrane proteins?

Model and methods. We simulate lipid membranes utilizing a flexible lipid model [18] and triple-strand rigid proteins [19] [Fig. 1(a)]. We use the model of Khoshnood et al. [19] and perform MD simulations of an NVT ensemble. Although different coarse grained models have been developed over years [20], the model adopted here has the ability to mimic the physical properties of lipid membranes. We express the position and velocity vectors of particles in the Cartesian (x, y, z) coordinate system whose origin is located at the center of our cubic simulation box. The x and y axes lie in the membrane plane and the z axis is perpendicular to that.

MD scales of length, time, mass and energy are $\sigma = 1/3$ nm, $\tau = 1.4$ ps, $N_{\rm avo}m = 36$ g/mol and $N_{\rm avo}\epsilon = 2$ kJ/mol, respectively. $N_{\rm avo}$ is the Avogadro's number. In all simulations, the dimensions of the box along the coordinates axes, L_x, L_y and L_z, are set to $L_x = L_y = L_z = 28.71\sigma$. The total number of particles equals $N = 15625$, which gives a fixed number density $\rho = 2/(3\sigma^3)$. Lees-Edwards boundary condition is employed to generate simple shear flow [21] with the shear rate $\dot{\gamma} = 0.03\tau^{-1}$. Other boundary conditions are periodic. The temperature is set to 324 K so that the system is safely above the gel to liquid phase transition temperature of different phosphatidylcholine lipid bilayers. Physical quantities are measured using a run-time of $\approx 5000\tau$. We compute the tension of our model membranes from $\zeta = \left[P_{zz} - (P_{xx} + P_{yy})/2 \right] L_z$ where $P_{\alpha\alpha}$ $(\alpha \equiv x, y, z)$
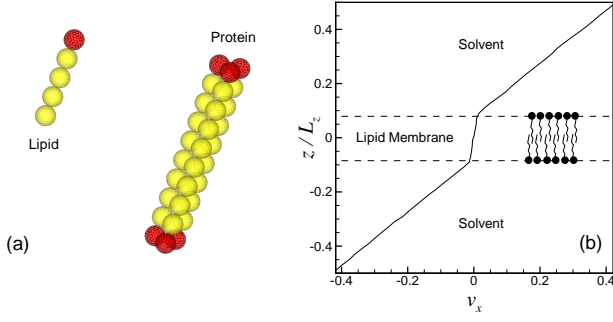
* mjalali@sharif.edu

FIG. 1. (a) The models of lipid and protein molecules. Red and yellow spheres are hydrophilic and hydrophobic particles, respectively. (b) Velocity profile of a sample solvent–membrane system under simple shear flow with $\dot{\gamma} = 0.03\tau^{-1}$.

are the components of the pressure tensor.

In this study we apply MSD to determine the diffusion properties of randomly moving particles. The diffusion coefficient is thus calculated using the Einstein expression

$$D_{\alpha\alpha} = \lim_{t\to\infty} \frac{1}{2Nt} \langle \sum_{i=1}^{N} [q_{i\alpha}(t) - q_{i\alpha}(0)]^2 \rangle, \qquad (1)$$

where $\alpha \in \{x, y, z\}$ and $q_{i\alpha}$ is the displacement due to the random motion of the ith particle in the α-direction. The summation in Eq. (1) is taken over the particles of the same type. From here on, we will drop the summation sign for brevity. The operator $\langle \cdots \rangle$ denotes the canonical average. Eq. (1) describes the regular Brownian motion when the MSD is linearly proportional to t. For anomalous diffusion one has

$$\langle [q_{\alpha}(t) - q_{\alpha}(0)]^2 \rangle = 2D_{\alpha\alpha}^a t^a, \qquad (2)$$

where a is the diffusion exponent and $D_{\alpha\alpha}^a$ is the fractional diffusion coefficient. The regimes with $0 < a < 1$ and $a > 1$ are subdiffusive and superdiffusive, respectively. To obtain smooth MSD curves, we evolve systems of 80 different initial conditions and report their ensemble-averaged diffusion coefficients and MSDs. The diffusion of lipids is investigated by tracing the motion of their head groups. Proteins are traced using their center of masses.

In equilibrium models the flux of particles is associated with their random motions, and any displacement is due to thermal fluctuations. In sheared membranes, however, there is a combination of streaming and diffusive fluxes. We thus need to distinguish and eliminate the streaming flux when calculating the MSD. Let us define the actual velocity components of the jth particle as $v_{j\alpha} = \langle v_\alpha \rangle + \tilde{v}_{j\alpha}$ where $\langle v_\alpha \rangle$ is the average streaming velocity, and $\tilde{v}_{j\alpha}$ is the peculiar velocity whose time integral gives the displacements in Eqs. (1) and (2). In equilibrium models, the average velocities $\langle v_\alpha \rangle$ vanish and we obtain $q_{j\alpha} = \int v_{j\alpha} dt = \int \tilde{v}_{j\alpha} dt$. With external shearing, the flow is always imposed in the x-direction. Therefore,

$v_{jy} = \tilde{v}_{jy}$ and $v_{jz} = \tilde{v}_{jz}$ are directly integrated to find the corresponding displacements. When the simulation box is uniformly filled with one type of particles (let us says solvent particles), one readily finds $\tilde{v}_{jx} = v_{jx} - z\dot{\gamma}$. In the presence of a lipid bilayer, the vertical velocity profile in the z-direction is no longer linear [see Fig. 1(b)]. Therefore, to obtain the MSD of lipids, we define $\langle v_x \rangle$ as the average velocity of the layer where the head groups of phospholipds reside, and obtain $q_{jx} = \int (v_{jx} - \langle v_x \rangle) dt$.

Diffusion of lipids. The lateral diffusion of lipids in equilibrium conditions is enhanced as the membrane tension increases [22, 23]. By turning on the shear flow, lipid molecules undergo an initial ballistic motion that transforms into an interval of subdiffusion with $a = 0.7$ [Fig. 2(a)]. The transient anomalous state has been observed in atomistic simulations [24] as well. After the transient anomalous diffusion and over longer time scales a normal diffusion with $a = 1$ is observed [Fig. 2(a)]. It is noted that we have found similar MSD profiles for lipid molecules in equilibrium and sheared systems, and in both cases lipids ultimately develop normal diffusion. Although Kneller et al. [25] reported a permanent subdiffusive behavior by the atomistic simulation of lipid membranes in equilibrium, experiments support a final regular diffusion regime, as we do, even in the presence of obstacles [26]. We conclude that the diffusion regime of lipid molecules is invariant with and without external shearing.

The diffusion coefficients obtained from the normal diffusion region of MSD plots, are larger for smaller shear rates. For example, for a membrane of $N_l = 600$ lipid molecules, we find $\zeta = (1.4846 \pm 0.2624)\sigma^2/\epsilon$, $D_{xx} = 0.001608\sigma^2/\tau$ and $D_{yy} = 0.001587\sigma^2/\tau$. For the same system under a shear flow of $\dot{\gamma} = 0.03\tau^{-1}$, the membrane tension drops to $\zeta = (0.8163 \pm 0.2727)\sigma^2/\epsilon$ and diffusion coefficients reduce to $D_{xx} = 0.001513\sigma^2/\tau$ and $D_{yy} = 0.001580\sigma^2/\tau$. The reason is that the membrane thickness increases for higher shear rates and the tension decreases without any change in the area per lipid [19]. Consequently, the fluidity of the membrane decreases and slows down the diffusion process. After applying the shear force, we find that D_{xx} drops for about 6 percent while D_{yy} remains almost constant [this is indistinguishable in Fig. 2(a)]. We speculate that the alignment of lipid chains with the flow breaks the isotropy and yields $D_{xx} \neq D_{yy}$. In the z-direction, perpendicular to the membrane plane, our MSD plots always show a confined motion as is expected.

Diffusion of proteins. We add rod-like proteins to the membrane, and simulate models with different protein concentrations that vary significantly from cell to cell. Since proteins increase the membrane tension as they perturb the distribution of lipids [19], we increase the number of lipids (proportional to proteins) to keep the membrane tensionless. In equilibrium and for a membrane with a single embedded protein, we can measure the diffusion coefficients $D_{\alpha\alpha}$ since the MSD of protein shows an ultimate regular diffusion. We find
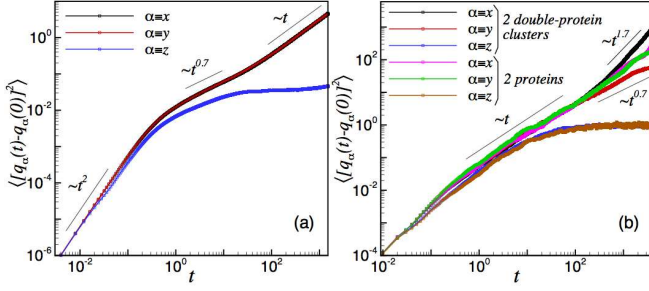
FIG. 2. (a) MSD of lipid molecules. The membrane is sheared and has 600 lipids. (b) MSD of protein molecules in a protein-embedded sheared model with 2 and 4 proteins, which correspond to 640 and 660 lipids, respectively.

$D_{xx} = 0.0253\sigma^2/\tau$ and $D_{yy} = 0.0254\sigma^2/\tau$, which are equivalent to $D_{xx} \approx D_{yy} \approx 2 \times 10^{-9}$ m^2/s. These values are larger than experimental values, by two orders of magnitude. The obvious reason is the effect of coarse graining that has reduced the interdigitation and friction between molecules, and allows for faster movements of particles. By putting the system under simple shear flow, proteins undergo Brownian motion when only two proteins are used [Fig. 2(b)]. One could anticipate this result, for single proteins cannot remarkably perturb the distribution of lipids, and change the diffusion properties of the membrane. With 4 proteins, however, we observe that they form two double-protein clusters (due to the depletion force), and exhibit a strong superdiffusive motion parallel to the flow. Fig. 2(b) shows how after $t \sim 100\tau$ the normal diffusion regime transforms to strong superdiffusion with $a = 1.7$ in the x-direction. Interestingly, this exponent is the same as the superdiffusion exponent found by Köhler et al. [14] for active diffusion of protein clusters by molecular motors. Because of crowding effect and increase in the concentration of proteins [1], our results show a subdiffusive behavior along the y axis with $a = 0.7$. Weigel et al. [9] observed $a = 0.8 \pm 0.1$ in experiments with channel proteins of human kidney cell, and Javanainen et al. [27] found $a = 0.75 \pm 0.15$ by molecular simulations of aggregating NaK channel proteins.

Let us define the local concentration of the head particles of lipid and protein molecules at the position $\boldsymbol{r}$ and time t as $f = \frac{1}{N_\mathrm{h}} \sum_{i=1}^{N_\mathrm{h}} [H(\delta_i) - H(\delta_i - \Delta)]$ where $\delta_i(t) = |\boldsymbol{r}_i(t) - \boldsymbol{r}|$, and $\boldsymbol{r}_i(t)$ is the position vector of the ith head particle. N_h denotes the total number of head particles in the monolayer, $H(\xi)$ is the Heaviside step function, and 2Δ is the typical size of the cross section of a protein cluster (or a protein–lipid complex). Our numerical experiments show $\Delta = 4\sigma$ is the best choice. We examine the trajectories of protein molecules and the spatial variation of the normalized distribution $\hat{f}(\boldsymbol{r}, \Delta, t) = (f - f_\mathrm{min})/(f_\mathrm{max} - f_\mathrm{min})$ to explain the physics of observed superdiffusion. Here f_min and f_max are the minimum and maximum values of f at a given
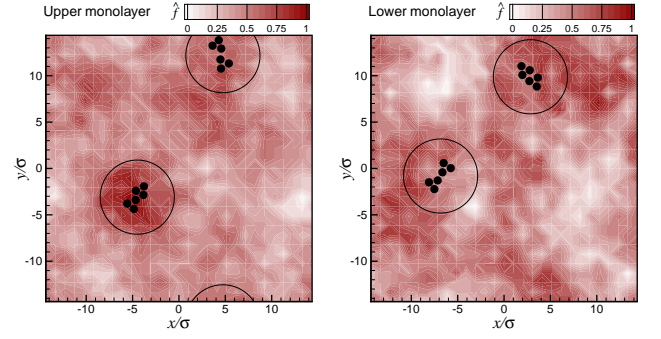

FIG. 3. The local concentration $\hat{f}(\boldsymbol{r}, \Delta, t)$ of head groups in the upper (left panel) and lower (right panel) leaflets of a sheared membrane. The head particles of proteins are shown by filled circles. Drawn circles have radii of Δ, and their centers lie at the centroid of the head particles of proteins. The flow is in the x^+ and x^- directions for upper and lower leaflets, respectively [cf. Fig. 1(b)]. The model has 660 lipids and two double-protein clusters.

time t. Fig. 3 demonstrates contour plots of $\hat{f}$ for the upper and lower monolayers at a randomly selected time.

Fig. 4(a) demonstrates the trajectories of a single protein molecule and two double-protein clusters, in equilibrium and sheared systems, respectively. The equilibrium trajectory corresponds to regular diffusion because it covers a definite area. In the sheared system trajectories show local isotropic wanderings followed by small-step jumps mainly in the flow direction. These successive jumps can be interpreted by inspecting the contour plots of $\hat{f}(\boldsymbol{r}, \Delta, t)$ over a long duration of time. The hydrophobic mismatch between protein clusters and the membrane disturbs the bilayer thickness and the arrangement of nearby lipids. Moreover, proteins are able to transport their neighboring lipids with them and behave as dynamic complexes [3, 4]. These two effects collaborate to create transient voids whose distribution can be described by $\hat{g} = 1 - \hat{f}$ (light shades in Fig. 3). When the bilayer is sheared, protein–lipid groups are pushed into the voids created by themselves or other groups/complexes and experience accelerated, and therefore, superdiffusive movements. It should be noted that during our simulations, the center of mass of the membrane and embedded proteins remains almost at the center of the coordinate system.

We have computed the probability distribution function (PDF) of protein displacements and plotted it in Fig. 4(b). A Gaussian function has been fitted to the data by setting its maximum to the maximum of PDF, and its variance is found using the full width at half minimum of PDF. The PDF exhibits a deviation from normal distribution and it has tails. We have also applied the Kolmogorov-Smirnov test [28] to confirm that the PDF is not a normal Gaussian. This is a clear indication of anomalous diffusion.

The ends of proteins are pulled in opposite directions by the two sheared solvent columns. An important ques-
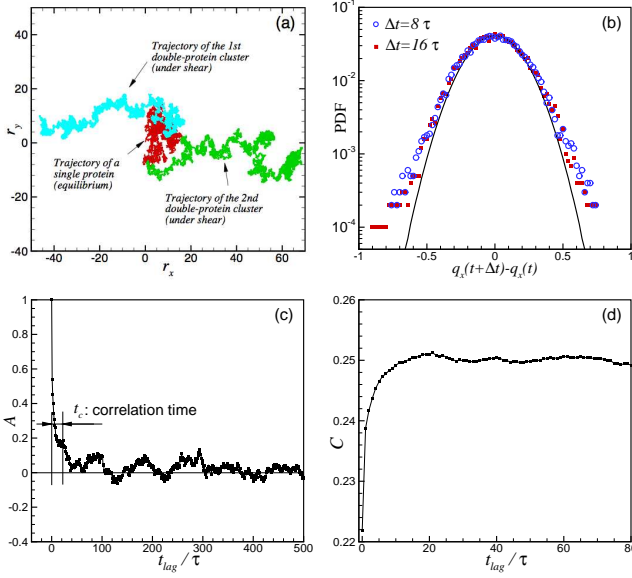
FIG. 4. (a) Trajectories of a single protein in equilibrium (red) and two double-protein clusters (cyan and green) under shear flow. (b) PDF for the displacements of a sample two-protein cluster. Solid line shows the best Gaussian function fitted to the data. (c) Autocorrelation function $A(t_{\text{lag}})$. The correlation time $t_c \approx 23\tau$ is defined at the point where $A(t_{\text{lag}})$ abruptly drops below 10% of its maximum. We have taken 1000 successive samples in the time domain, with increments of 1τ, to compute A. (d) Cross-correlation function $C(t_{\text{lag}})$. The integrals in C have been taken using a grid of 29×29 in the xy-plane and 1000 successive points, with steps of 1τ, in the time domain.

tion is why do protein clusters prefer to jump into the voids when the membrane is sheared? We have a simple explanation for this behavior: Two ends of proteins attract lipids from two different layers of the membrane. Thus, the symmetry in the distribution of the upper and lower protein-bound lipids is likely to break. Moreover, the shear force is exerted by the solvent on both the lipid and protein heads. The mentioned symmetry breaking thus leads to different force components at the upper and lower ends of protein–lipid complexes, and they will jump into a void in the direction specified by the broken symmetry. To quantify this process, we take a sample two-protein cluster and define $\boldsymbol{r}_u$ and $\boldsymbol{r}_l$ as the center of masses of its protein heads in the upper and lower leaflets, respectively. We then compute $\xi(t_i) = \hat{f}(\boldsymbol{r}_u, \Delta, t_i) - \hat{f}(\boldsymbol{r}_l, \Delta, t_i)$, which is proportional to the net shear force exerted on the cluster at the time

step t_i: the local effective area in contact with a solvent column is determined by the number of head particles, and the shear force is calculated by multiplying the effective contact area by the shear rate and viscosity. $\xi(t_i)$ will be zero if the concentrations of the head particles of lipids are identical around the two heads of the cluster. Defining $\bar{\xi}$ as the average of $\xi(t_i)$, the autocorrelation function

$$A(t_{\text{lag}}) = \frac{\sum_i \left[\xi(t_i + t_{\text{lag}}) - \bar{\xi} \right] \cdot \left[\xi(t_i) - \bar{\xi} \right]}{\sum_i \left[\xi(t_i) - \bar{\xi} \right]^2}, \quad (3)$$

plotted in Fig. 4(c) carries interesting information about the shear force experienced by the cluster: the correlation time $t_c \approx 23\tau$ shows a sustained accelerated motion of the cluster over $t_0 < t \lesssim t_0 + t_c$, independent of the initial time t_0. Moreover, the oscillatory decaying profile of $A(t_{\text{lag}})$ shows a random symmetry breaking in the sense of deterministic chaos [29, §5.3.4]. The existence of a correlation time can also be verified by studying the cross-correlation function $C(t_{\text{lag}}) = \int dt \int d\boldsymbol{r} \, \hat{f}(\boldsymbol{r}, \Delta, t+t_{\text{lag}}) \cdot \hat{g}(\boldsymbol{r}, \Delta, t)$ over one of the leaflets. Fig. 4(d) shows that $C(t_{\text{lag}})$ of the upper leaflet steeply rises from $t_{\text{lag}} = 0$ and peaks at $t_{\text{lag}} \approx 21\tau$, which is the earliest time span that protein–lipid complexes need to occupy their nearest voids. This is quite consistent with the acceleration time scale of protein clusters predicted by the autocorrelation function $A(t_{\text{lag}})$. For $t_{\text{lag}} \gtrsim 21\tau$ the cross-correlation function remains almost flat because the size of a void is always bigger than the distance that a protein cluster travels during $t \sim \mathcal{O}(t_c)$.

Conclusions. Cell responses to stimuli are fast due to enhanced mobility of protein receptors. Consider our findings, superdiffusion of proteins under shear flow can play a dominant role in the process of signaling in endothelium cells, RBCs, liposomes used for targeted drug delivery and other sheared membranes. We note that since the length and shape of proteins and their ability in attracting neighboring lipids controls the sizes of voids —there was no other mechanism in our models for void generation— superdiffusion properties reported in this study are not universal and they highly correlate with the properties of embedded proteins. Simulations using detailed structures of lipids and proteins are needed to better assess the superdiffusive behavior in realistic cell membranes. Experimental exploration of our results can be done using single particle tracking [30] which can give the MSD of proteins directly.

[1] J. A. Dix, and A. S. Verkman, Annu. Rev. Biophys., **37**, 247 (2008).

[2] S. Wieser, J. Weghuber, M. Sams, H. Stockinger, and G. J. Schuetz, Soft Matter, **5**, 3287 (2009).

[3] P. S. Niemelä, M. S. Miettinen, L. Monticelli, H. Hammaren, P. Bjelkmar, T. Murtola, E. Lindahl, and I. Vattulainen, J. Am. Chem. Soc., **132**, 7574 (2010).

[4] A. Prasad, J. Kondev, and H. A. Stone, Phys. Fluids,

19, 113103 (2007).

[5] S. Ramadurai, A. Holt, L. V. Schafer, V. V. Krasnikov, D. T. S. Rijkers, S. J. Marrink, J. A. Killian, and B. Poolman, Biophys. J., **99**, 1447 (2010).

[6] Y. Gambin, M. Reffay, E. Sierecki, F. Homble, R. S. Hodges, N. S. Gov, N. Taulier, and W. Urbach, J. Phys. Chem. B, **114**, 3559 (2010).

[7] G. Guigas and M. Weiss, Biophys. J., **94**, 90 (2008).

[8] F. Bartumeus, J. Catalan, U. L. Fulco, M. L. Lyra, and G. M. Viswanathan, Phys. Rev. Lett., **88**, 097901 (2002).

[9] A. V. Weigel, B. Simon, M. M. Tamkun, and D. Krapf, Proc. Natl. Acad. Sci., **108**, 6438 (2011).

[10] J.-H. Jeon, H. M.-S. Monne, M. Javanainen, and R. Metzler, Phys. Rev. Lett., **109**, 188103 (2012).

[11] S. Ramadurai, A. Holt, V. Krasnikov, G. van den Bogaart, J. A. Killian, and B. Poolman, J. Am. Chem. Soc., **131**, 12650 (2009).

[12] T. H. Solomon, E. R. Weeks, and H. L. Swinney, Phys. Rev. Lett., **71**, 3975 (1993).

[13] F. Lechenault, R. Candelier, O. Dauchot, J. P. Bouchaud, and G. Biroli, Soft Matter, **6**, 3059 (2010).

[14] S. Köhler, V. Schaller, and A. R. Bausch, Nat. Mater., **10**, 462 (2011).

[15] M. Chachisvilis, Y. Zhang, and J. A. Frangos, Proc. Natl. Acad. Sci., **103**, 15463 (2006).

[16] P. J. Butler, G. Norwich, S. Weinbaum, and S. Chien, Am. J. Physiol. Cell Physiol., **280**, C962 (2001).

[17] M. A. Haidekker, N. L'Heureux, and J. A. Frangos, Am. J. Physiol. Heart Circ. Physiol., **278**, H1401 (2000).

[18] R. Goetz and R. Lipowsky, J. Chem. Phys., **108**, 7397 (1998).

[19] A. Khoshnood, H. Noguchi, and G. Gompper, J. Chem. Phys., **132**, 025101 (2010).

[20] S. J. Marrink, H. J. Risselada, S. Yefimov, D. P Tieleman, and A. H. de Vries, J. Phys. Chem. B, **111**, 7812 (2007).

[21] M. P. Allen, and D. J. Tildesley, *Computer Simulation of Liquids*, (Oxford University Press, Oxford, UK., 1991).

[22] J. Neder, B. West, P. Nielaba, and F. Schmid, J. Chem. Phys., **132**, 115101 (2010).

[23] H. S. Muddana, R. R. Gullapalli, E. Manias, and P. J. Butler, Phys. Chem. Chem. Phys., **13**, 1368 (2011).

[24] E. Flenner, J. Das, M. C. Rheinstadter, and I. Kosztin, Phys. Rev. E, **79**, 011907 (2009).

[25] G. R. Kneller, K. Baczynski, and M. Pasenkiewicz-Gierula, J. Chem. Phys., **135**, 141105 (2011).

[26] M. J. Skaug, R. Faller, and M. L. Longo, J. Chem. Phys., **134**, 215101 (2011).

[27] M. Javanainen, H. Hammaren, L. Monticelli, J.-H. Jeon, M. S. Miettinen, H. Martinez-Seara, R. Metzler, and Ilpo Vattulainen, Faraday Discuss., (2013).

[28] W. H. Press, S. A. Teukolsky, W. T. Vetterling, and B. P. Flannery, *Numerical Recipes: The Art of Scientific Computing*, 3rd Edition, (Cambridge University Press, 2007)

[29] J. H. Argyris, G. Faust, and M. Haase, *An exploration of chaos: an introduction for natural scientists and engineers*, (North-Holland, 1994)

[30] J. M. Crane, and A. S. Verkman, Biophys. J., **94**, 702 (2008).